Received: 10 October 2019 | Revised: 5 November 2020 | Accepted: 8 November 2020

DOI: 10.1002/we.2596

RESEARCH ARTICLE

WILEY

Wind turbine event detection by support vector machine

Congcong Hu | Roberto Albertani

School of Mechanical, Industrial and Manufacturing Engineering, Oregon State University, Corvallis, Oregon, USA

Correspondence
Roberto Albertani, School of MIME, Oregon State University, Corvallis, OR, USA.
Email: roberto.albertani@oregonstate.edu

Funding information
Office of Energy Efficiency and Renewable Energy, Grant/Award Number: DE-EE0007885

Abstract

Considering the increase in the deployment of wind energy conversion systems, improving the coexistence between wind turbines and wildlife with an efficient method for blade impact assessment is of primary importance. Automated blade-impacts on potential wildlife monitoring can support the development and operations of wind farms. A substantial challenge is represented by the typical case of impacts vibrations signature embedded in the operational vibrations of the wind turbine. A heterogeneous multisensor system for automatic eagle detection and deterrent, including an automatic blade-event detection module, was developed providing the necessary field data. An automated blade event detection system, based on support vector machine, a form of machine learning, was developed and tested. Training of the algorithm was performed using features extracted from vibration signals and energy distribution graphs obtained from numerical simulations of blade impacts. Performance of the method, evaluated using numerical simulations at different levels of signal-to-noise ratios, relative to artificial impacts, showed the best results when trained using combined raw vibration signal and time marginal integration graphs, exhibiting an overall *accuracy* of 93% at SNR = 6. The proposed model was tailored for improving specificity (i.e., false negative error), a critical aspect for endangered species events. Performance of the trained algorithm evaluating field data exhibited an improvement in impact detection from a visually identifiable rate of 42% to true positive prediction rate of 75%. The system could perform, with appropriate training, diverse functions as components health monitoring or lighting strike automatic monitoring.

KEYWORDS
birds, environment, impact monitoring, health monitoring, machine learning, support vector machine, vibration sensors, wind turbine

1 | INTRODUCTION

One of the major ecological objectives associated with the deployment of wind farms is the improvement of the coexistence of birds and bats with wind turbines.[1-5] Automated blade impacts on potential wildlife monitoring can support the development and operations of wind farms. While blade collisions rates have been investigated and reported,[6,7] traditional mortality estimates still rely on methods such as long-term visual

[Correction added on 4 March 2021, after first online publication: URL for peer review history has been corrected.]

observation and carcass survey.[8-11] Those methods however are characterized by inherent uncertainties caused mainly by scavengers, low deployment of human observers, and the nature of the environment like presence of thick grass, shrubs, or on water. Under the aforementioned conditions, the estimated mortality rates could contain significant differences from reality.[10]

One approach for effective and low-cost automatic detection of bird/bat collision with wind turbines is to apply continuous vibration and noise monitoring on blades by the implementation of vibrational or acoustic sensing devices. The conceptual design of a multisensor system that provides both temporal and spatial coverage capacities for autodetection of bird collision events was carried out at Oregon State University (OSU) based on prior research on bird collision monitoring systems.[12,13] Vibrations and structural-borne noise data were acquired during field testing on utility-scale wind turbines. Artificial collision events were created by launching tennis balls into moving blades using compressed-air cannon. Preliminary results showed that it is feasible to detect an impact using common vibration sensors by visual inspection. Relatively simple automatic algorithms were applied in the case of high signal-to-noise ratios (SNR).[12] However, vibration signals that contain low-intensity impacts embedded in relatively high background noise are characterized by low SNRs, exhibiting low rate or no success in detection. In such cases, more advanced signal processing algorithms need to be developed and tested using experimental data.

Vibration-based monitoring techniques are well developed and widely adopted on modern wind turbines for the main purpose of structural health monitoring (SHM).[14,15] Vibration sensors such as piezoelectric diaphragms and accelerometers are commonly applied for the analysis of dynamic structural response during turbine operations.[16] A significant effort has been devoted by researchers for the detection of faults in rotating parts such as blades, bearings, and gearbox under dynamic loads, by identifying its characteristic features in the vibration signal. In such case, signals caused by the defects will have a periodic characteristic. However, when in the occurrence of an abnormal one-time event, typically, a blade strike or a lighting strike, the resulting effect is a nonperiodic signal. Currently, there are no practical existing methods/techniques for automatic nonperiodic event detection. Moreover, a substantial challenge is represented by the case of impacts vibrations signature being embedded and hidden in the operational vibrations of the wind turbine, a typical case of normal operations.

This paper presents a robust method for automatic detection of nonperiodic event under the general framework of SHM. Instead of traditional statistical analysis involved in SHM, a predictive model is constructed by implementation of support vector machine (SVM), one of the most widely applied machine learning methods for general classification problems such as condition monitoring and fault diagnosis.[17] The proposed method extracts features from vibrations signals acquired on wind turbine blades and associated energy distribution graphs. Training of SVM is achieved by running the algorithm on a significant number of impact simulations. Preliminary results obtained by testing the predictive model trained by SVM using simulations of blade impact[18] showed an increasing performance as the SNR increases, as expected. This paper explains further developments in the SVM algorithm training methodologies by conducting simulated studies. Finally, a SVM predictive model was constructed, and its performance was evaluated using field data on a commercial 1.5-MW wind turbine with and without impacts on the blades.

2 | METHODS

2.1 | Support vector machine

SVM is a supervised machine learning method introduced by Cristianini[17] and Boser et al.[19] It is widely applied to specific fault diagnosis of different types of machinery.[20] The method, well known for classification of periodic-type events, was originally defined and applied to nonperiodic events such as blade impacts with foreign objects. Using time histories of vibrations and structure-borne noise on wind turbine blades, a binary classification problem including two classes of labeled events for training is defined. SVM then is employed to construct a predictive model for new nonlabeled events.[18]

Given a sample dataset $(x_i, y_i)_{i=1}^{N}$, x_i denotes the ith vector in the input space X and y_i is the label associated with x_i. A hyperplane, in the form of

$$f(x) = w^T x + b = 0, \tag{1}$$

where w is the weight vector and b is the bias, is established to divide the input space X into two classes: positive ($f(x) > 0$) and negative ($f(x) < 0$). Maximum margin criterion is applied to find the optimized hyperplane, which gives the maximum distance between the nearest data and plane, as illustrated in Figure 1. Misclassification is allowed by introducing slack variables $\xi_i > 0$ and error penalty (also called soft-margin constant) $C > 0$. The problem can be expressed by the following constrained optimization problem:

$$\begin{aligned} &\text{Minimize } \frac{1}{2}\|w\|^2 + C\sum_{i=1}^{n}\xi_i \\ &\text{subject to } y_i(w^T x_i + b) \geq 1 - \xi_i, \end{aligned} \tag{2}$$

which is also known as soft-margin SVM.

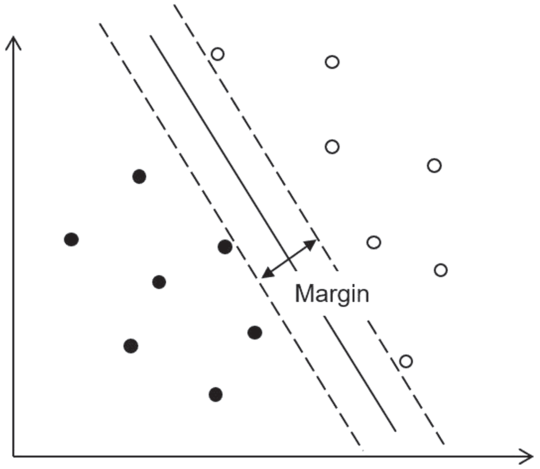

FIGURE 1 Illustration of linear classifier in two-dimensional feature space given by maximum margin criterion

For data that are nonlinearly separable in the input space X, the input vector x_i can be mapped into a higher feature space F by mapping function $\Phi(x)$, making them linearly separable. Since explicitly mapping input vectors from the lower dimensional space into the higher dimensional space can result in quadratic complexity, kernel function $K(x_i,x_j) = \Phi^T(x_i) \cdot \Phi(x_j)$ is introduced to solve the issue by skipping the step of explicitly mapping.[17] The following four basic kernels are most commonly used:

- linear: $K(x_i,x_j) = x_i^T x_j$,
- polynomial: $K(x_i,x_j) = (\gamma x_i^T x_j + r)^d, \gamma > 0$,
- radial basis function (RBF): $K(x_i, x_j) = exp(-\gamma \|x_i - x_j\|^2), \gamma > 0$,
- sigmoid: $K(x_i,x_j) = tanh(\gamma x_i^T x_j + r)$.

2.2 | Application to impact detection

The application of the methods described above for automatic impact detection on wind turbine blades starts with the collection of raw time histories collected by the sensors installed on the wind turbine blades and then processed by continuous wavelet transform (CWT), followed with integrating CWT with respect to time, producing the energy distribution graph, which is also defined as the time marginal integration (TMI) graph.[18] The flow chart of the proposed method is shown in Figure 2. A total number of 18 statistical features are extracted from the raw signals and TMI graphs, as listed in Table 1. These time-domain features are commonly applied in vibration monitoring methods for SHM.[21-24]

The next step is model training using extracted features. The performance of the trained SVM model in this work is mainly influenced by two parameters: soft-margin constant (C), which controls the penalty assigned to classification/margin errors, and RBF kernel parameter (γ), which significantly affects the decision boundary. The optimum values of C and γ need to be determined for the optimal model of the best prediction capability. This optimization procedure is carried out through standard experimental setup of grid search evaluated by cross validation technique. In k-fold cross-validation, training data are divided into k equal subsets. Each subset is tested using the model trained by the remaining $k-1$ subsets so that each instance in the whole training set is predicted once. Cross-validation error (CV_error), defined as

$$\mathrm{CV_error} = \frac{\text{Number of incorrectly predicted instances}}{\text{Total number of instances in the training set}}, \tag{3}$$

is used to evaluate the performance of trained model with selected parameters. In this work, the predictive model is trained by 10-fold cross-validation with parameters C and γ optimized by grid search in a grid of 2^{-10}–2^{10} to achieve the minimum cross validation error.

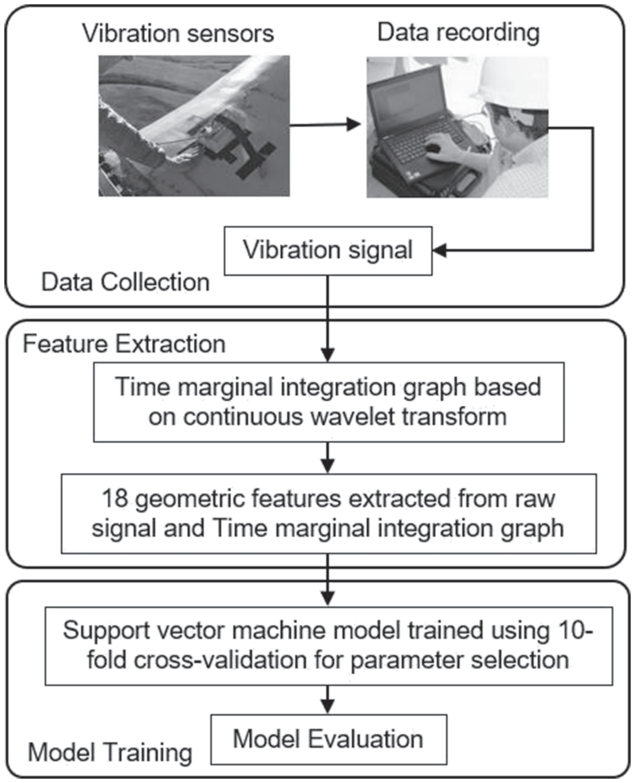

FIGURE 2 Flow chart of proposed method for automatic impact detection on wind turbine blade

TABLE 1 List of extracted features

No.	Feature from raw signal	No.	Feature from TMI graph
1	Kurtosis	10	Kurtosis
2	Skewness	11	Skewness
3	Mean	12	Mean
4	RMS	13	RMS
5	Variance	14	Variance
6	Peak	15	Peak
7	Impulse factor	16	Impulse factor
8	Shape factor	17	Shape factor
9	Crest factor	18	Crest factor

3 | SIMULATED STUDIES

To verify the validity of the SVM predictive model applied to impact detection, simulation experiments were conducted before its application to field experimental data. Simulations of independent events with and without impact components were performed. Demonstration of the advantage of TMI-based features was carried out. The performance of the model was further evaluated by the receiver operating characteristics (ROC) curve.

3.1 | Impact simulation

In the simulation, each independent training example is constructed by combining a single impact signal and the background noise. The single impact signal is defined as

$$s(t) = \begin{cases} 0 & t<0 \\ exp\left(-\frac{\xi}{\sqrt{1-2\xi^2}} \cdot 2\pi ft\right) \cdot sin(2\pi ft) & t \geq 0 \end{cases}, \quad (4)$$

where ξ is the damping coefficient, $\frac{\xi}{\sqrt{1-2\xi^2}}$ is the damping attenuation characteristics of impact response, and f is the sampling frequency.[25] The background noise is simulated using Gaussian white noise characterized by its mean and root mean square (RMS) value. Signals are characterized by different SNR levels, which depend on impact signal intensities and background vibrations. The SNR is defined as follows:

$$\text{SNR} = 20log_{10}\frac{A_{\text{impact}}}{A_{\text{noise}}}, \quad (5)$$

where A denotes the RMS amplitude. Figure 3 illustrates simulated training example signals of the pure impact with $\xi = 0.007$ and $f = 512$ Hz, Gaussian white background noise with zero-mean and 0.05 RMS, and the resulting combined waveform, respectively. The impact of SNR = 1.5, which occurred at time = 0.5 s, was embedded in a noisy signal. For each level of SNRs (12 different levels from SNR = 0.5 to SNR = 6 with an increment of 0.5), a total number of 10,000 independent examples (5000 with impact and 5000 without impact) were simulated.

3.2 | Performance evaluation

The SVM model was trained with 10-fold cross-validation and evaluated by overall accuracy[18] and ROC curve. The overall accuracy, defined by

$$\text{Overall accuracy} = \frac{TP+TN}{TP+TN+FP+FN}, \quad (6)$$

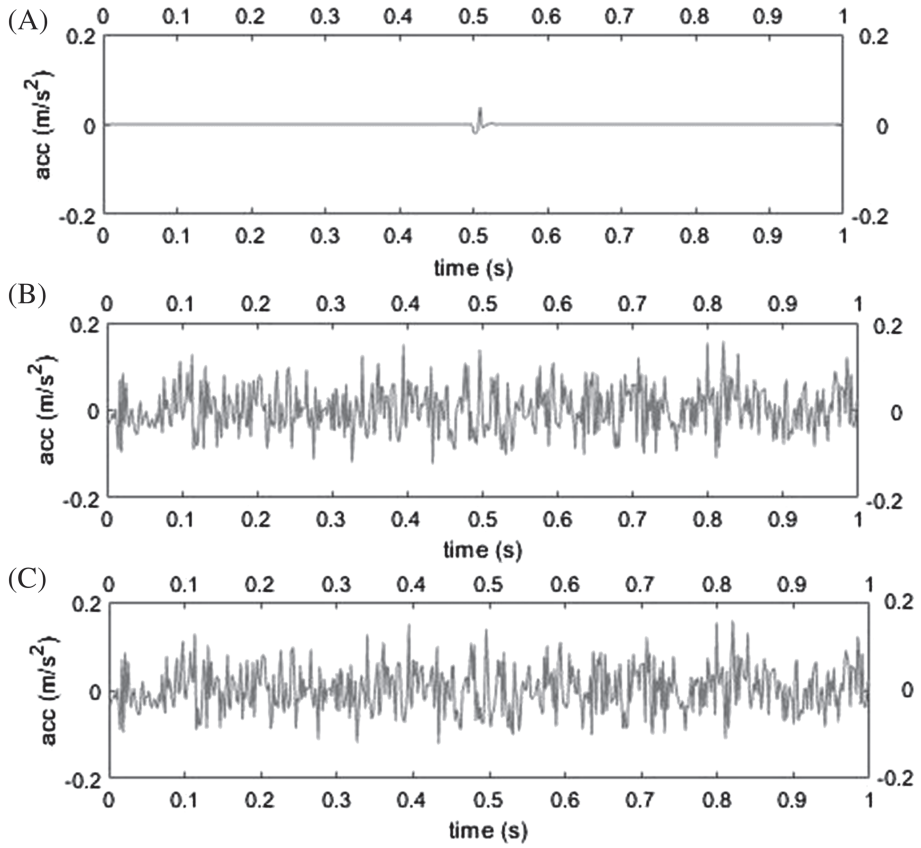

FIGURE 3 Result of an example of the construction of a simulated blade impact with the waveform of combined signal with SNR = 1.5: (A) Single impact with $\xi = 0.007$ and $f = 512$ Hz, (B) Gaussian white background noise with zero-mean and 0.05 root mean square, and (C) resulting mixed signal

where *TP*, *TN*, *FP*, and *FN* are true positive, true negative, false positive, and false negative events, respectively, represents the general performance of the predictive model. To select an appropriate kernel function, the performance of four commonly used kernels on simulated data is illustrated in Table 2. As can be noted, the RBF and sigmoid kernels both outperformed linear and polynomial with similar overall accuracy at different levels of SNRs. Since the RBF kernel performs slightly better in higher SNRs and it is generally preferred in most situations,[17] it is applied in the present work.

Figure 4 shows the relationships between SNR and accuracy of three different models (i.e., model trained by raw features only, TMI features only, and combined raw and TMI features). It was expected that the overall accuracy of all models increases as the SNR increases, exhibiting linear regression relationships. When SNR < 2 (i.e., the impact energy is too small), all models are considered as underfitting since an approximate of 50% detection rate in binary classification indicates nothing more than a random guess. Figure 4 also demonstrates the advantage of TMI-based features. For instance, at SNR = 6, while the accuracy of the model trained by TMI features was 91.46%, the model trained by raw features only showed a much lower accuracy of 80.32%. The model trained by combined features showed the best performance (93.98% in accuracy), which indicates a modest increase in respect to the model trained by TMI features only.

ROC plot is a graphical plot that shows relative trade-off between true positive rate and false positive rate.[26] It is obtained by plotting the sensitivity against 1 – specificity. The sensitivity, also known as the true positive rate, is a measure of the fraction of actual positives which have been classified as such. The specificity, also known as the true negative rate, measures the fraction of actual negatives correctly classified as such. They are mathematically expressed as

$$\text{Sensitivity} = \frac{TP}{TP + FN}, \tag{7}$$

$$\text{Specificity} = \frac{TN}{TN + FP}. \tag{8}$$

The obtained ROC plot for each selected level of SNR is shown in Figure 5. It can be noted from Figure 5 that as SNR increases, the points move towards the top-left corner, which represents a perfect model with 100% rate in both sensitivity and specificity. Random guess boundary was also proved by the ROC plot for SNR < 2. In the three cases of SNR = 0.5, 1, and 1.5, the data points are close to the diagonal line (i.e., 50% random guess line), indicating the model is inefficient and underfitting. Additionally, considering a real case of impact detection between an

TABLE 2 Performance of different kernels on simulated data

SNR	Linear	Polynomial	RBF	Sigmoid
3	56.43%	49.91%	59.35%	59.55%
4	65.42%	51.24%	72.98%	71.10%
5	73.40%	56.68%	83.80%	83.15%
6	92.46%	84.20%	95.80%	94.72%

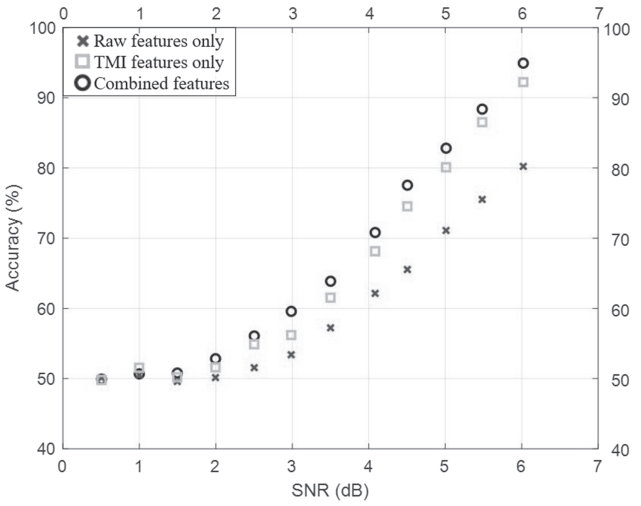

FIGURE 4 Impact simulation results showing relationship between SNR and accuracy for three different cases of model training

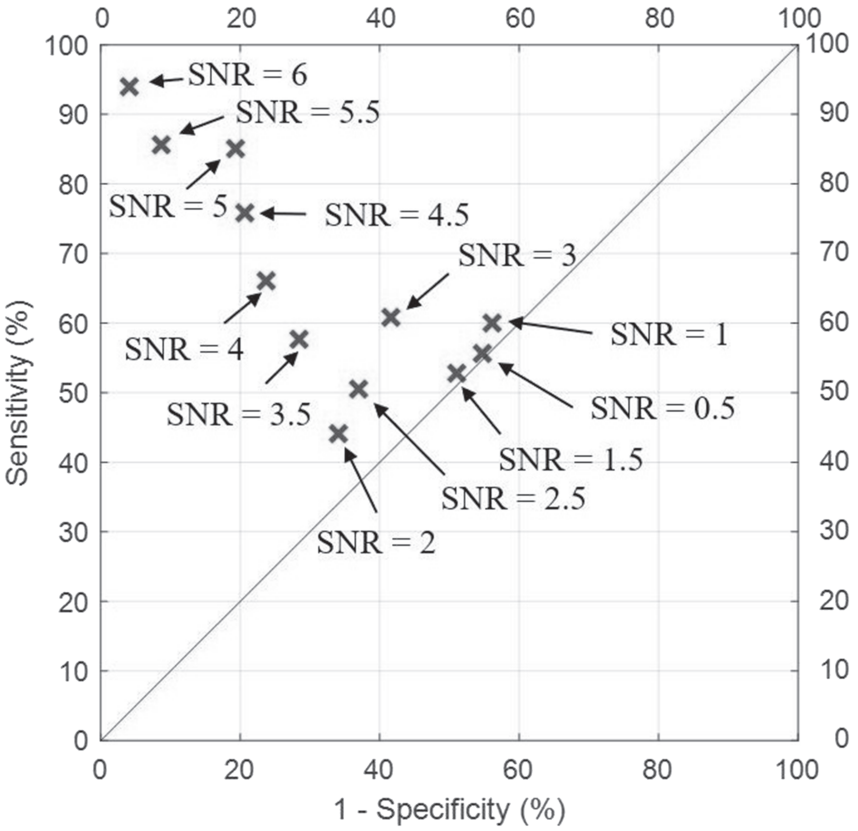

FIGURE 5 ROC graphs showing classification performance of the proposed method using simulation data

FIGURE 6 Eagle detection, deterrent, and blade event detection system diagram

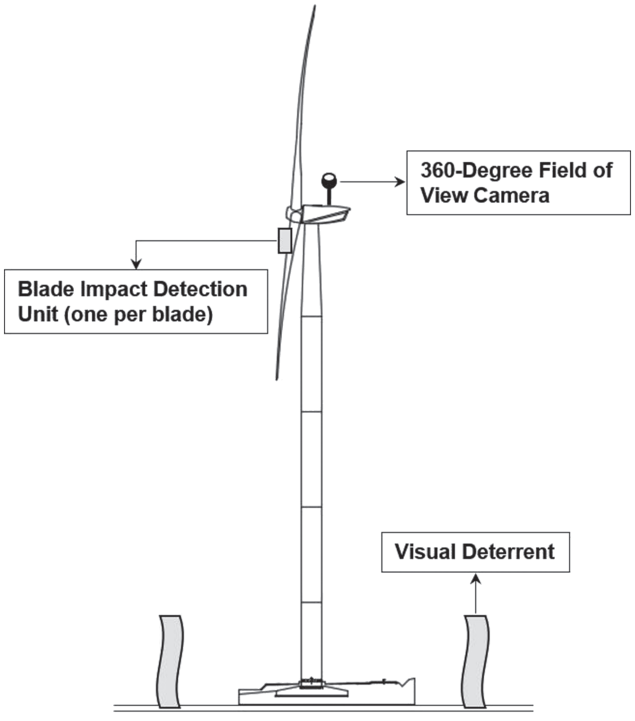

endangered species and wind turbine blade, the occurrence of false negative is considered more critical than the occurrence of false positive. In this respect, the specificity is considered more critical than sensitivity. Although SNR = 5.5 has approximately the same sensitivity (i.e., false positive error) as SNR = 5, the model is superior in improving specificity (i.e., false negative error).

4 | EXPERIMENTAL EVALUATION

4.1 | System overview

A heterogeneous multisensor system with specific capabilities of eagle detection and identification, eagle deterrent, and blade collision detection has been recently developed.[27] The system mainly consists of three modules as shown in Figure 6. The monitoring of the airspace surrounding a wind turbine is performed by the first module, a 360° field-of-view commercial camera. The camera module provides real-time feedback about the presence of moving objects, eagle identification, and their flight paths with respect to the turbine structure. Once a moving object is detected with sufficient number of pixels, eagle identification can be carried out by computer vision deep-learning techniques.[27] In a positive event of eagle flying towards the wind turbine, kinetic inflatable visual deterrents on the ground will be deployed automatically. The third module is a weather-proof blade impact detection (BID) unit installed at the root of each blade as shown in Figure 7. The module includes vibration sensors, an accelerometer and a contact microphone, providing continuous structural vibration monitoring used for blade collision detection. The InvenSense MPU-9250 MEMS triple axis accelerometer, forming an inertial measurement unit (IMU), is rigidly attached inside the BID unit with two axes (*Y* and *Z*) being in-plane in respect of the blade and parallel to the chord line and *X* axis off-plane. It provides the capability of recording acceleration data in the full-scale range of ±16 *g* with a rated frequency response of 4–4000 Hz and a sensitivity scale factor of 2048 LSB/*g*. The contact microphone (CUI Inc. CEB-27D44) is a piezoelectric diaphragm that consists of a piezoelectric ceramic plate with an electrostatic capacitance of 16,000 at 1 kHz. Being attached to the blade surface using adhesive tapes, the deformation of the piezoelectric ceramic plate caused by surface vibrations induces the electric charge. The accelerometer and contact microphone were set to acquire data at sampling rates of 512 and 1000 Hz, respectively. These sampling rates were specified based on the processing capability of current hardware for real-time collision monitoring.[12,28,29] In addition, the BID unit contains a on-blade surveillance camera that provides visual images for potential taxonomic identification.

4.2 | Field testing summary

The overall system functionality and reliability were validated by field tests at the National Renewable Energy Laboratory (NREL) National Wind Technology Center (NWTC) in Boulder, CO, and at the North American Wind Research and Training Center (NAWRTC) at the Mesalands Community College in Tucumcari, NM, both on a General Electric (GE) 1.5-MW wind turbine. Artificial impacts were created by launching tennis balls and small potatoes using a custom compressed-air cannon.[12,13] Sample plots of raw vibration recordings from the three blades on the GE 1.5 MW at the NWTC are illustrated in Figure 8. The top three time histories represent the voltage time histories recorded by the contact microphones, and bottom three represent *X* axis (i.e., out-of-plane axis) accelerations recorded by the accelerometers. The tests were under low-wind speed conditions and with the rotor in slow wind milling rotation. The figures show the impact occurring on Blade #1 was clearly visible due to the relatively high SNRs, 14.1 and 4.4 for contact microphone and accelerometer, respectively. Due to the low background vibration noise and high impact intensity, sensors on Blade #2 and Blade #3 were also able to capture this impact with relatively lower SNRs. The impact cannot be easily discerned from noise and signal spikes from Blade #2 signal from the contact microphone. Cases of data with extremely high noise in the signals or multiple random spikes were classified as N/A.

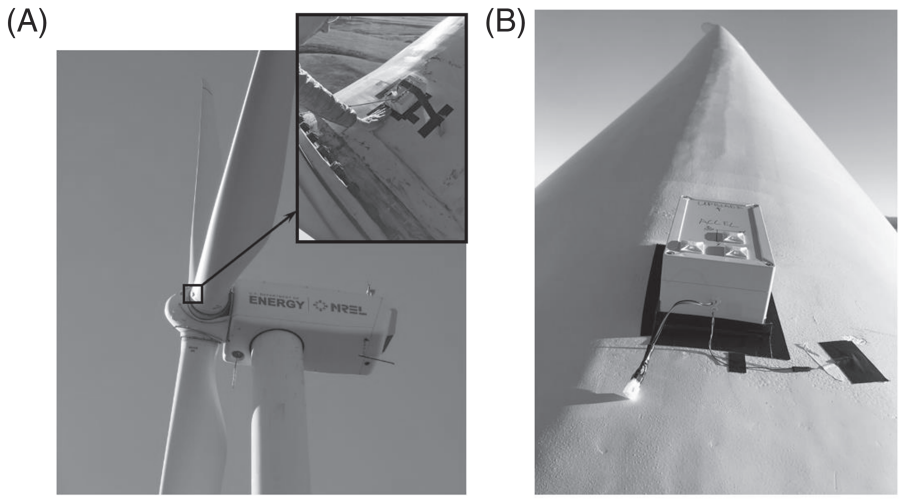

FIGURE 7 Blade impact detection unit installed at the root of each blade on the GE 1.5 MW at the NREL National Wind Technology Center

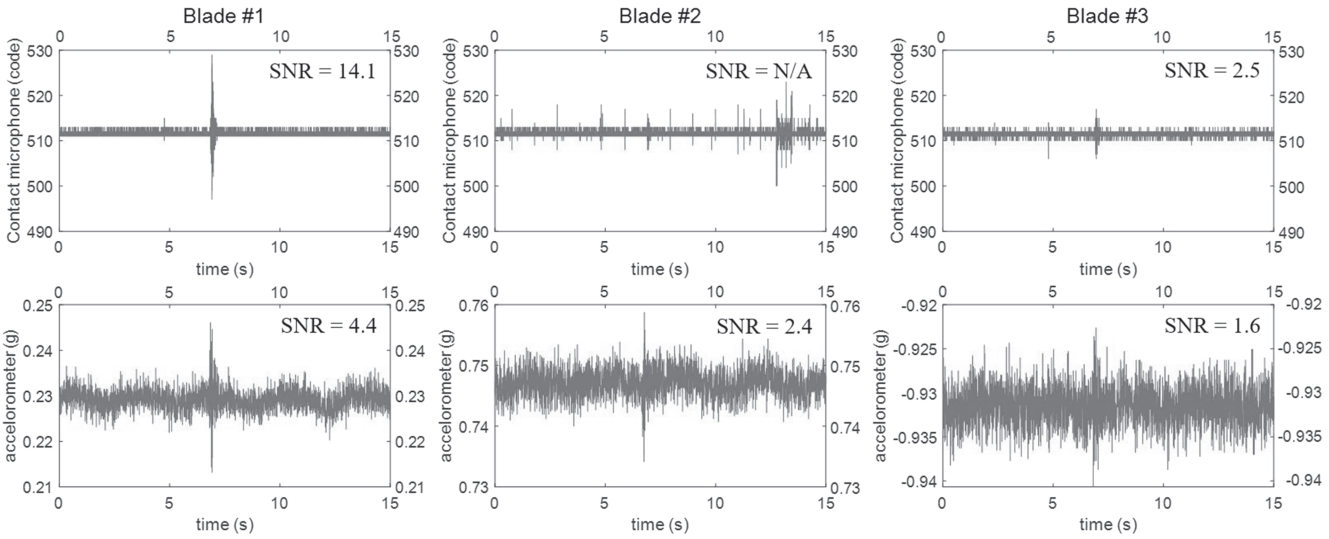

FIGURE 8 Vibration signals from contact microphones (upper plots) and accelerometers (lower plots) with impact occurred on Blade #1

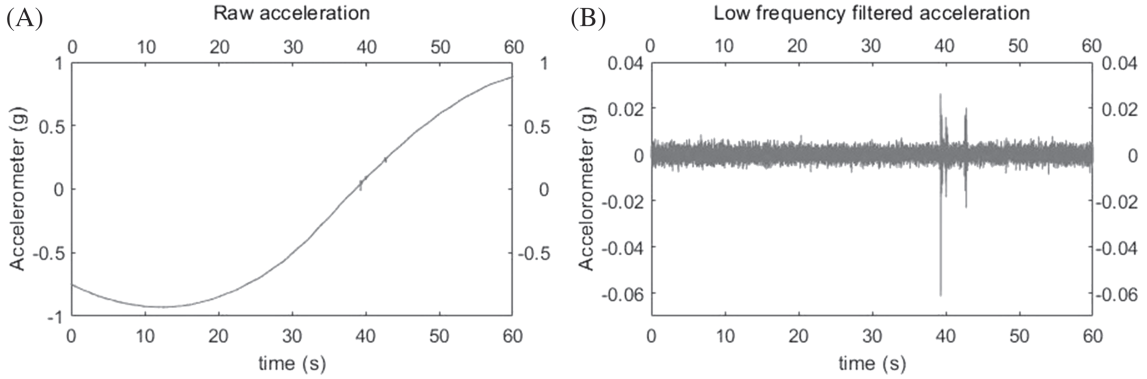

FIGURE 9 Illustration of a high-pass filter. (A) Raw acceleration signal recorded by the accelerometer installed on Blade #2 during an impact. (B) After the application of a high-pass filter with cutoff frequency of 5 Hz, low-frequency components caused by blade rotation was eliminated

In summary, 13 artificial impacts with tennis balls at NWTC and 13 at NAWRTC were successfully obtained and manually annotated during wind turbines normal operation. Preliminary inspection showed that 11 over the total 26 impact events can be visually identified by any of the recorded raw signals with calculated SNRs in a range between 1.3 and 25.4 with an average of 6.3. Field notes show that most of the identified impacts occurred at the leading edge of the turbine blade thus at a relatively high kinetic energy, while impacts concealed by signal noise and with significantly low SNRs were usually located closer to the rotor shaft at low kinetic energy.

4.3 | Application

4.3.1 | Data preparation and model training

Characteristically for a supervised machine learning method, a SVM predictive model requires a substantial number of training examples from all classes to modify and optimize its nonprobabilistic linear classifier. In real applications, the vibration sensors would be installed on turbine blades for a sufficient long period of time to obtain vibrations with and without impacts. Since the blade impacts obtained during field tests were not sufficient for an efficient training of the predictive model, a large number of signals with and without impacts were mathematically simulated for training purposes. The simulated signals, characterized by RMS of the background noise and SNR of the impact, were created to replicate the characteristics of the actual signals.

Preliminary inspection on all impact signals indicated a higher reliability of accelerometer signals since contact microphone data exhibited random noise such as multiple spikes shown in Figure 8 Blade #2, which can be misclassified as false positive impacts. The three-axis acceleration

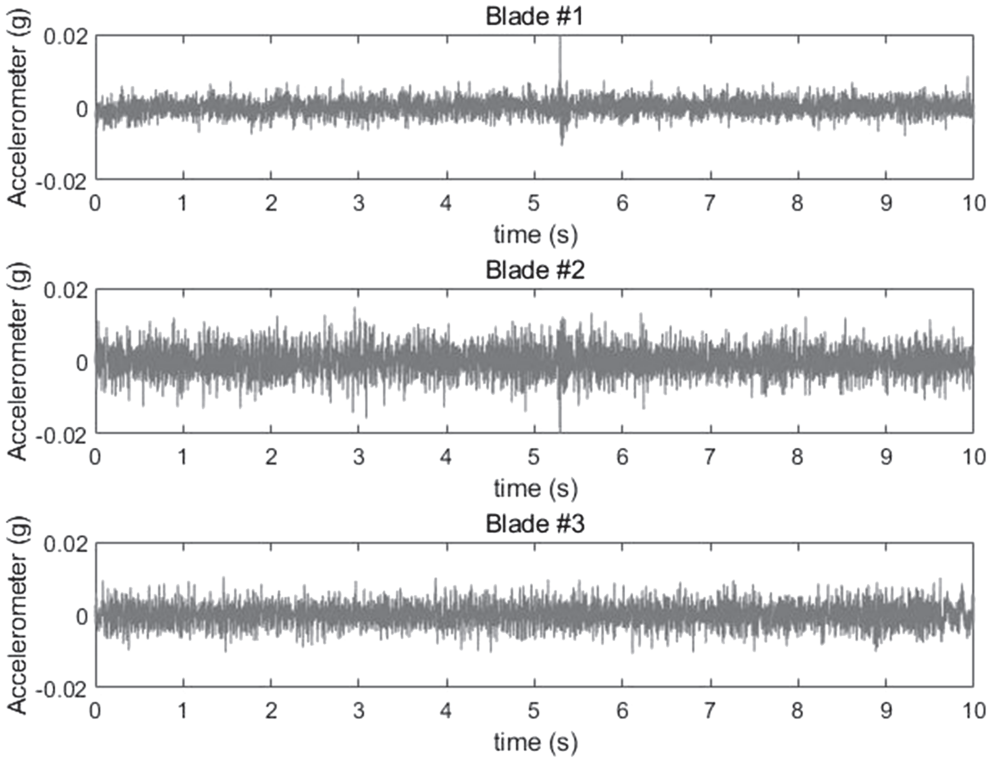

FIGURE 10 Illustration of actual acceleration signals used in model evaluation. (A–C) Raw vibration signals recorded by the accelerometers installed on three respective blades during one impact event, Impact #2

TABLE 3 Predictive labels of the 13 actual impacts by the predictive model

Impact #	Blade #1	Blade #2	Blade #3	Overall accuracy
1	1	N/A	N/A	100%
2	1	1	−1	99%
3	1	−1	−1	97%
4	1	1	−1	99%
5	1	−1	−1	98%
6	1	1	1	Approximately 50%
7	N/A	1	1	99%
8	N/A	N/A	N/A	N/A
9	1	1	1	Approximately 50%
10	1	N/A	N/A	Approximately 50%
11	1	N/A	N/A	99%
12	1	N/A	N/A	99%
13	−1	1	−1	98%

data showed a wide variation of RMS and SNR due to different test sites, changing weather and turbine operating conditions. To avoid attributes in larger numeric ranges dominating those in lower ranges, the out-of-plane *X* axis acceleration data from the NAWRTC tests with similar signal properties were selected for valid evaluation of the proposed method. The 13 sets of actual impact signals from NAWRTC, each containing three *X* axis acceleration signals from the three respective blades, were selected for the evaluation of the SVM predictive model. A high-pass filter with cutoff frequency of 5 Hz was applied to acceleration signals to eliminate low-frequency components caused by blade rotation, as illustrated in Figure 9. All signals were offset to zero to avoid numerical difficulties in calculation. The calculated RMS values range from 0.0020 to 0.0027 with an average SNR of 2.7 for all identifiable impacts.

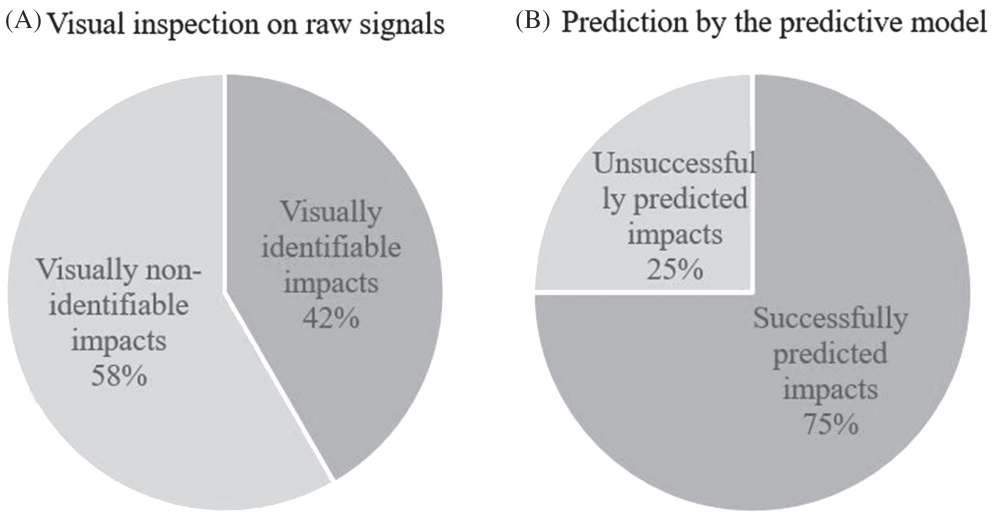

FIGURE 11 Results in percentage of identifiable impacts by: (A) visual inspection and (B) the constructed predictive model

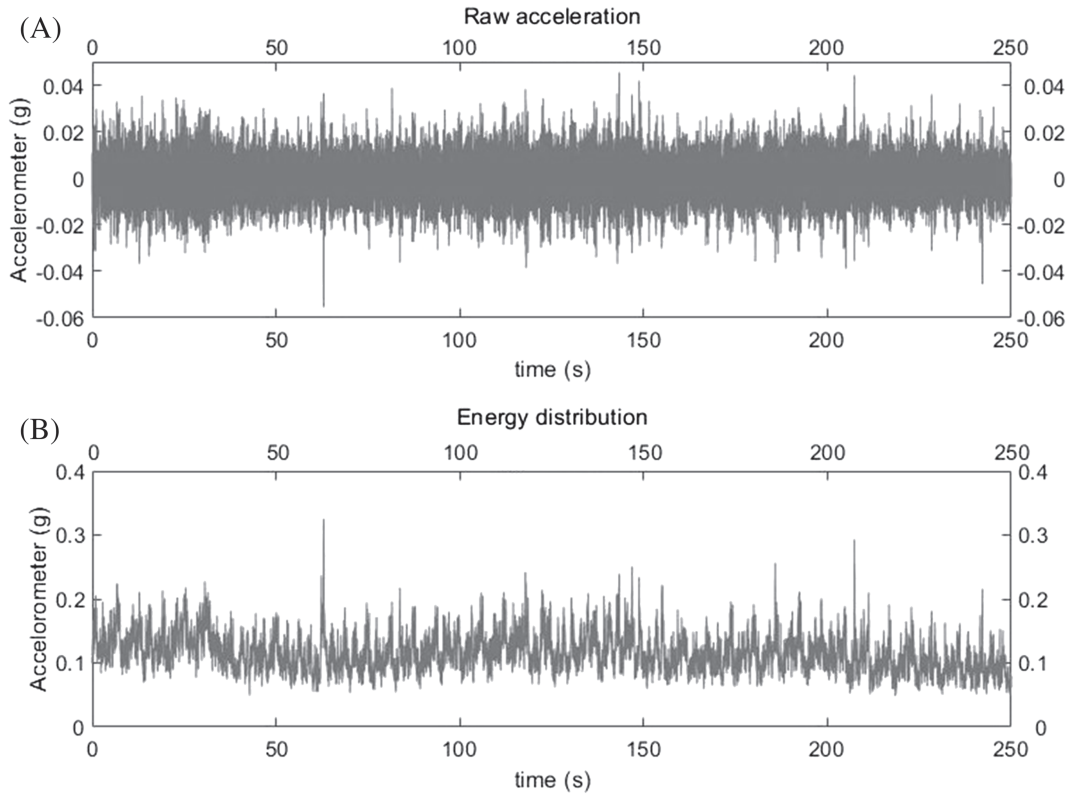

FIGURE 12 Graphs of (A) raw acceleration time histories and (B) energy distribution of Impact #12 on Blade #1. The impact was visually non-identifiable but was successfully predicted by the predictive model

A total number of 10,000 independent examples (5000 with impact and 5000 without impact) were simulated with zero-mean, RMS of 0.0027 g and a fixed SNR of 2.7. 10-s signal were simulated at sampling frequency of 512 Hz; thus, each instance contains 5120 data points for data processing. The predictive model was trained using those examples by 10-fold cross-validation with parameters C and γ optimized by grid search in a grid of 2^{-10}–2^{10}. It was observed when C and γ are equal to 0.169 and 0.129, respectively, the optimal model has the minimum cross validation error that equals to 0.79%.

4.3.2 | Results

It was determined that testing the predictive model, obtained as explained above, with real vibrations signals was critical; thus, the constructed model was evaluated using 13 actual impacts. Figure 10 illustrates one set (i.e., three instances during one impact event, 5120 data points each) of the raw vibration data used for model evaluation. For testing purpose, 1000 extra independent examples (500 with impact and 500 without impact) were simulated by the same parameters as used in the training dataset simulation and were added to each actual impact to construct a rich testing dataset. This step provides a larger base of testing examples for the overall accuracy evaluation, which is necessary in determining if a model is reliable or underfitting. The labels of the 13 actual impacts as predicted by the proposed model including overall accuracy are listed in Table 3. Although all actual impacts were predicted as impacts by any of the three-axis acceleration, Impacts #6, #9, and #10 showed significantly lower overall accuracy (approximately 50%), indicating the model is underfitting; hence, their results were considered invalid. The reason for low accuracy was attributed to high signal noise level. Figure 11 shows graphically the overall results of our validation runs. Excluding Impact #8, 75% of the actual impacts (nine out of 12) were successfully predicted, including those impacts signal concealed by the background noise, compared to 42% of the actual impacts (five out of 12) identified by visual inspection or detectable by simpler algorithms. Figure 12 illustrates a sample of a non-identifiable signal that was successfully predicted to contain an impact with an overall accuracy of 99%.

5 | CONCLUSIONS

This study demonstrates the feasibility of the proposed SVM model for detection of blade impact signals concealed in background noise using vibration data collected by conventional sensors (accelerometer and contact microphone) installed on wind turbine blades. Field tests were performed on commercial wind turbines in operating conditions with addition of artificial impacts of tennis balls on blades. Considering the collected data base of confirmed artificial impacts, 11 out of 26, with an average calculated SNR of 6.3, were identified by visual inspection. Those impacts could be alternatively automatically detected by simple automatic algorithms. Simulated operational vibrations with and without impact showed that the proposed SVM model formulated from features extracted from raw and TMI signal has been found to be effective in automatic impact detection in low SNR when the impact is embedded in the background vibration noise, and virtually invisible from inspection. Field impacts augmented by a number of mathematically simulated impacts, at different levels of SNRs, including at extremely low levels of SNRs, showed that the proposed SVM model can effectively detect and classify an abnormal one-time (nonperiodic) event as an impact with sufficient accuracy for relatively low levels of SNRs. Considering a SNR ≥ 6, the overall accuracy can be higher than 93%. Results also showed approximately 50% of accuracy for SNR < 2.0, which indicates the model limit reaching random guess in a binary classification problem. Random guess boundary was also proved by the ROC plot illustrating model results close to the diagonal random guess line for SNR < 2. Comparison between predictive models formulated by three different feature sets showed the best results for the model trained using combined features extracted from both raw vibration signal and TMI graph. TMI-only feature however showed results close to the combination of the two while using raw features only exhibited the lowest performance. Finally, the predictive model trained by simulated signals was evaluated using field data from NAWRTC. Results showed an overall true positive impact detection of 75% compared to 42% of the actual impacts identified by visual inspection or detectable by simpler algorithms, validating that concealed (not visible) impacts can be successfully identified by the proposed predictive model. Alternative training of the same algorithm can perform different tasks as blade SHM, lighting strike or hail impact automatic monitoring. The system is designed to be turbine-agnostic; thus, it can be installed and implemented at any time of the turbine operational life or deployment.

6 | FUTURE WORK

As concluded, the proposed model with the current training is not effective for extremely low levels of SNR < 2. Potential improvements of the system include the following:

- Algorithm optimization for real time operations;
- Establish new features with stronger correlations with the characteristics of an impact event need in the presence of significant background vibrations noise;
- Increase field data collection to improve model training and possibly identifying new features;
- Installing multiple sensors at different positions per blade and on nacelle and apply sensor fusion techniques to improve impact signal detection. Optimization studies with the objective of establishing the minimum number of vibration sensors on blades for optimum performance and minimum cost could also be beneficial.

ACKNOWLEDGEMENTS

The authors would like to acknowledge, and thank, the U.S. Department of Energy Office of Energy Efficiency and Renewable Energy for financial support under contract DE-EE0007885 Wind Energy—Eagle Impact Minimization Technologies and Field Testing Opportunities. The authors are also grateful to the staff at the NREL National Wind Technology Center and at the North American Wind Research and Training Center at Mesalands Community College for their support and guidance during the system's field tests and data acquisition on their wind turbines.

CONFLICT OF INTEREST

The authors declare no potential conflict of interests.

PEER REVIEW

The peer review history for this article is available at https://publons.com/publon/10.1002/we.2596.

ORCID

Roberto Albertani https://orcid.org/0000-0003-1284-8087

REFERENCES

1. Bailey H, Brookes KL, Thompson PM. Assessing environmental impacts of offshore wind farms: lessons learned and recommendations for the future. *Aquat Biosyst*. 2014;10(1):8.
2. Thomsen K. *Offshore Wind: A Comprehensive Guide to Successful Offshore Wind Farm Installation*. 2nd ed. Elsevier Science; 2014:1-404. https://www.elsevier.com/books/offshore-wind/thomsen/978-0-12-410422-8
3. Zohbi GA, Hendrick P, Bouillard P. Evaluation of the impact of wind farms on birds: the case study of lebanon. *Renew Energy*. 2015;80:682-689.
4. Grodsky SM, Behr MJ, Gendler A, et al. Investigating the causes of death for wind turbine-associated bat fatalities. *J Mammal*. 2011;92(5):917-925.
5. Loss SR, Will T, Marra PP. Estimates of bird collision mortality at wind facilities in the contiguous United States. *Biol Conserv*. 2013;168:201-209.
6. Sovacool BK. Contextualizing avian mortality: a preliminary appraisal of bird and bat fatalities from wind, fossil-fuel, and nuclear electricity. *Energy Policy*. 2009;37(6):2241-2248.
7. Marques AT, Batalha H, Rodrigues S, et al. Understanding bird collisions at wind farms: an updated review on the causes and possible mitigation strategies. *Biol Conserv*. 2014;179:40-52.
8. Korner-Nievergelt F, Brinkmann R, Niermann I, Behr O. Estimating bat and bird mortality occurring at wind energy turbines from covariates and carcass searches using mixture models. *PLOS ONE*. 2013;8(7):e67997.
9. Parisé J, Walker TR. Industrial wind turbine post-construction bird and bat monitoring: a policy framework for canada. *J Environ Manag*. 2017;201:252-259.
10. Smallwood KS. Long search intervals underestimate bird and bat fatalities caused by wind turbines. *Wildl Soc Bull*. 2017;41(2):224-230.
11. Kunz T, Arnett EB, Cooper BM, et al. Assessing impacts of wind-energy development on nocturnally active birds and bats: a guidance document. *J Wildl Manag*. 2007;71(8):2449-2486.
12. Hu C, Albertani R, Suryan RM. Wind turbine sensor array for monitoring avian and bat collisions. *Wind Energy*. 2018;21:255-263.
13. Flowers J, Albertani R, Harrison T, Polagye B, Suryan RM. Design and initial component tests of an integrated avian and bat collision detection system for offshore wind turbines. In: Marine Energy Technology Symposium; 2014; Seattle, WA. http://hdl.handle.net/10919/49197
14. Ciang CC, Lee J-R, Bang H-J. Structural health monitoring for a wind turbine system: a review of damage detection methods. *Meas Sci Technol*. 2008;19(12):122001. https://doi.org/10.1088/0957-0233/19/12/122001
15. Yang W, Tavner PJ, Crabtree CJ, Feng Y, Qiu Y. Wind turbine condition monitoring: technical and commercial challenges. *Wind Energy*. 2014;17(5):673-693. https://onlinelibrary.wiley.com/doi/abs/10.1002/we.1508
16. Martinez-Luengo M, Kolios A, Wang L. Structural health monitoring of offshore wind turbines: a review through the statistical pattern recognition paradigm. *Renew Sustain Energy Rev*. 2016;64:91-105. http://www.sciencedirect.com/science/article/pii/S1364032116301976
17. Cristianini N. *An Introduction to Support Vector Machines: And Other Kernel-Based Learning Methods*. Cambridge University Press; 2000. ISBN 0-521-780-019-5.
18. Hu C, Albertani R. Machine learning applied to wind turbine blades impact detection. *Wind Eng*. 2019;44:325-338.
19. Boser BE, Guyon IM, Vapnik VN. A training algorithm for optimal margin classifiers. In: Haussler D, ed. *Proceedings of the 5th Annual Workshop on Computational Learning Theory (COLT'92)*. Pittsburgh, PA, USA: ACM Press; 1992:144-152.
20. Widodo A, Yang BS. Support vector machine in machine condition monitoring and fault diagnosis. *Mech Syst Sign Process*. 2007;21(6):2560-2574. http://www.sciencedirect.com/science/article/pii/S0888327007000027
21. Kumar A, Kumar R. Time-frequency analysis and support vector machine in automatic detection of defect from vibration signal of centrifugal pump. *Measurement*. 2017;108:119-133.
22. Vanraj, Singh R, Dhami SS, Pabla BS. Development of low-cost non-contact structural health monitoring system for rotating machinery. *Royal Soc Open Sci*. 2018;5(6):172430. https://royalsocietypublishing.org/doi/abs/10.1098/rsos.172430
23. Das S, Saha P, Patro S. Vibration-based damage detection techniques used for health monitoring of structures: a review. *J Civil Struct Health Monit*. 201604;6:477-507.
24. Goyal D, Pabla B. The vibration monitoring methods and signal processing techniques for structural health monitoring: a review. *Archiv Comput Methods Eng*. 201503;23:585-594.
25. Liu R, Yang B, Zhang X, Wang S, Chen X. Time-frequency atoms-driven support vector machine method for bearings incipient fault diagnosis. *Mech Syst Sign Process*. 2016;75:345-370.
26. Yonelinas AP. Receiver-operating characteristics in recognition memory: evidence for a dual-process model. *J Exp Psychol*. 1994;20(6):1341-1354.

27. Albertani R, Johnston M, Todorovic S, Huso M, Katzner T. Eagle detection, identification and deterrent, with blade collision detection for wind turbines. In: Wind Wildlife Research Meeting XII. AWWI. St Paul, MN: AWWI; 2018:90-92.
28. Ghoshal A, Sundaresan MJ, Schulz MJ, Pai PF. Structural health monitoring techniques for wind turbine blades. *J Wind Eng Ind Aerodyn*. 2000;85(3): 309-324. http://www.sciencedirect.com/science/article/pii/S0167610599001324
29. Bassett K, Carriveau R, Ting DSK. Vibration response of a 2.3 MW wind turbine to yaw motion and shut down events. *Wind Energy*. 2011;14(8): 939-952. https://onlinelibrary.wiley.com/doi/abs/10.1002/we.457

How to cite this article: Hu C, Albertani R. Wind turbine event detection by support vector machine. *Wind Energy*. 2021;1–14. https://doi.org/10.1002/we.2596